Journal of Materials Science and Engineering A 10 (3-4) (2020) 65-75
doi: 10.17265/2161-6213/2020.3-4.004

Study of the Temperature of Cerebral Arterial Blood Flow, for the Characterization of the Degree of Stenosis: Application to Stroke

J. R. Tsafack Nzifack[1], J. S. Mabekou Takam[1], R. Moutou Pitti[2], M. Fogue[3] and P. K. Talla[1]

1. Unitéde Recherchede Mécaniqueetde Modélisationdes Systèmes Physiques (UR2MSP), Universitéde Dschang, Dschang 237, Cameroun

2. Universitéde Clermont Ferrand, SIGMA Clermont, Institut Pascal, F63000, Clermont-Ferrand 33, France

3. Unitéde Recherche d'ingénierie des systèmes industriels et de l'Environnement (LISIE), IUT Fotso Victorde Bandjoun 237, Cameroun

Abstract: Based on the biological heat transfer equation of Penne, the internal temperature distribution of the biological tissue was studied, taking into account the evolution of stenosis and hematocrit. The one-dimensional simplifying cylindrical heat equation of the biological living tissues in permanent regime was solved by the FDM (finite difference method) and analytically, to assess the temperature change under the variation of stenosis, hematocrit, *K* (thermal conductivity), kinematic viscosity, generation of metabolic heat and the heat transfer coefficient. The main results show that the temperature increases as the stenosis and hematocrit increase in size; and the secondary results show that the heat transfer coefficient and the *K* lower the body temperature while metabolic heat generation increases body temperature. This is in accordance with the literature.

Key words: Temperature, Penne's equation, stenosis, hematocrit.

1. Introduction

With the advancement of clinical medicine in thermal diagnosis of diseases, it is very important to understand thermal phenomena and the behavior of biological body temperature. One approach is to study the distribution of temperature in biological tissue. However, precise thermal analysis of biological tissue is difficult because they include conduction, convection, radiation, internal metabolism, evaporation, phase change and the regulation of the inherent temperature. Not only is the tissue heterogeneous and anisotropic, but the mechanisms also maintain body temperature, such as blood flow and metabolic heat generation. Recently, the development of research shows that the problem of heat transfer in biological tissues becomes a complex problem. But there are several discussions without conclusion in this area. Thus Pennes [1] proposed a simple linear mathematical model to describe the thermal interaction between human tissue and perfused blood, and the effect of metabolism. He measured the radial temperature in the forearm by drawing thin thermocouples through the arms of nine elongated subjects. This was based on experimental observation. Using this experimental concept, the models [2-8] have discussed thermal behavior in various constant parameters with human tissue layers. The distribution of temperature takes over in the blood and arterial tissues. Ref. [9] found an analytical solution of heat diffusion equation for brain tissue with negligible effect on blood flow and metabolic heat generation. Ref. [10] studied the abnormal thermoregulation model in the human dermal part. He also studied the temperature distribution in the steady state and in the unstable state in three layers of the dermal part. Ref. [11] studied the effect of the

Corresponding author: Pierre Kisito Talla, Ph.D., professor, research field: mechanics of materials.

thermal parameters of the dermal part in living cylindrical tissues. For the different models which have been investigated in literature, none of them considered the effect of hematocrit and stenosis which strongly influence the flow regime. In the present work, we are going to use the model in Ref. [1] used by Ref. [11], by coupling with hematocrit and stenosis to better control the variation of the temperature. Furthermore, we shall analyze the partitioning effect of hematocrit and the evolution of atherosclerosis on variation temperature variation. Here, we neglected the axial and angular direction and considered only the stationary state model of radial direction. The numerical FDM (finite difference method) and analytical results obtained are presented graphically and compared to the results of Ref. [11, 12] by applying the appropriate values of the physical and physiological parameters. The solution obtained can be used for the measurement of thermal parameters, the reconstruction of the temperature field and thermal diagnosis and in the treatment which maximizes the therapeutic effect while minimizing undesirable side effects. It may also be useful to design medical devices to operate within a special range of heating and cooling temperature rates, such as Ref. [12], thus for the prediction of cerebrovascular diseases.

2. Materials and Methods

2.1 Modelisation of Temperature

Over the past years, many researchers have developed different models with different views. The mathematical model used for the transfer of bio-heat is based on the Penne equation. Pennes [1] is preferable for studying the heat transfer between the blood and the tissues which also associates the metabolism effect and the blood perfusion. The modified Pennes equation is written as:

$$\rho c \frac{\partial T}{\partial t} = \nabla(k\nabla T) + w_b c_b \rho_b (T_a - T) + q_m \qquad (1)$$

where ρ, c, k are the density (kg/m^3), the specific heat (J/kg·℃) and the K (thermal conductivity) of tissue, respectively. w_b is the blood perfusion rate per unit volume (kg/s·m^3). c_b is the specific blood, q_m is the metabolic heat generation per unit volume (w/ m^3), T_a represents the temperature of arterial blood (℃) and T is the tissue temperature (℃). Based on the Pennes equation, the one-dimensional mathematical model was used to describe the heat transfer from living cylindrical tissues, in the stationary state, is presented below [11, 13].

$$\frac{1}{r}\frac{d}{dr}\left(r\frac{dT}{dr}\right) + \frac{w_b c_b \rho_b}{k}(T_a - T) + \frac{q_m}{k} = 0 \qquad (2)$$

The model is axial symmetric, so the boundary conditions are described as [11, 13]:

$$\begin{cases} r = 0\,, \dfrac{dT}{dr} = 0 \\ r = R\,, -k\dfrac{dT}{dr} = h_A(T - T_\infty) \end{cases} \qquad (3)$$

where R is the radius of the concerned tissue, h_A is the coefficient of heat transfer which accounts for the effects of both convection and radiation on the surface of the tissue, T_∞ is the ambient temperature.

2.2 Stenosis Modeling

Stenoses are characterized by a lesion of lipid infiltration, called an athermous plaque which develops on the internal surface of the arterial vessel (Fig. 1) and which blocks blood circulation and hematocrit (Fig. 2).

2.3 Characterization of Different Values of Reynold

To characterize the different Reynold values at the different stages of stenosis, we concentrated our mine in the work of Rizzini [15], which during its simulation calculated the Reynolds number (Re). The Re is a dimensionless quantity which is useful for determining whether the flow is laminar or turbulent: if it is greater than a critical value, the flow is turbulent, if it is less, the flow is laminar. In general, the Re is defined by the flowing formulation

$$\mathrm{Re} = \frac{\rho_b \vartheta d}{\mu_b} \qquad (4)$$

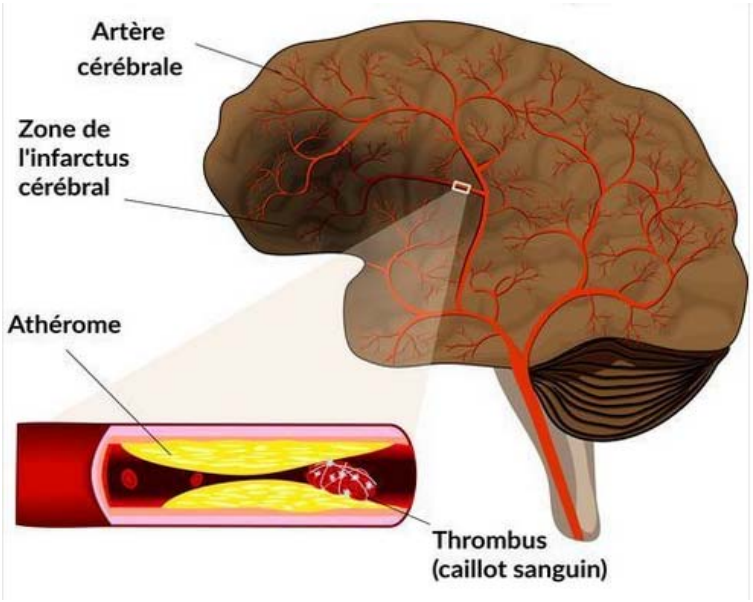

Fig. 1 Illustration of a plaque that blocks blood circulation.
Source: https://www.doctissimo.fr/html/sante/encyclopedie/sa_1583_ischemie_cereb.htm.

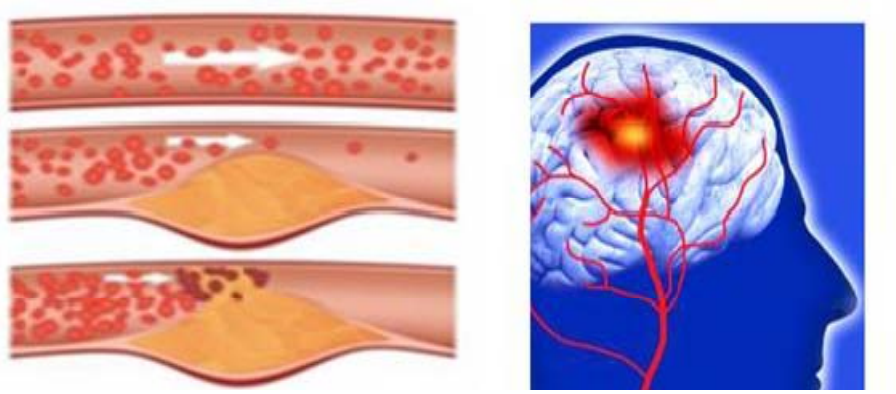

Fig. 2 Circulation of hematocrit in different stage of stenoses [14].

where ρ_b is the blood density, d is the diameter of the vessel, ϑ is the mean blood velocity throughout the vessel and it can be expressed as the ratio between the mean incoming flow (Q) and the inlet area (A):

$$\vartheta = \frac{Q}{A} = \frac{4Q}{\pi d^2} \quad (5)$$

where μ_b is the blood viscosity that is expressed using a simplified formulation of the Einstein relationship and is given by the following formula:

$$\mu_b = \mu_p(1 + 2.5H_t) \quad (6)$$

where μ_p represents plasma viscosity.

For low value of shear rate, blood behaves like pseudoplastic fluids and this behavior occurs for $H_t >$ 12%. This is due to the presence of fibrinogen which determines the aggregation of the red blood cells into "rouleau", generally mode up by fewer tens of erythrocytes, increasing blood viscosity. Since these parameters were known, Re was calculated at rest condition both for the non-stenotic model and in correspondence to the diameter of 3 stenoses, to see if

Table 1 Different stages of artery conditions with correspondence to Reynolds values determined by Rizzini [15] at rest condition $Q_{\text{rest}} = 60$ mL/min.

Different stage of artery condition	Non-stenotic model	30% stenosis	50% stenosis	75% stenosis
Re	334.04	482.27	675.15	1,350.33

these three degrees of stenosis may promote a laminar flow or cause a turbulent flow. The values obtained by Ref. [15] are reported in Table 1.

2.4 Final Model Formulation

In this section, we will couple the bio-heat model with the stenos model. Introducing Eq. (6) into Eq. (4), we will have:

$$\mathrm{Re} = \frac{\rho_b \vartheta d}{\mu_p(1 + 2.5H_t)} \tag{7}$$

Using Eq. (7), we obtain the new blood density:

$$\rho_b = \frac{\mu_p(1 + 2.5H_t)\mathrm{Re}}{\vartheta d} \tag{8}$$

Now let us introduce Eq. (8) into Eq. (2) to have a final expression of our model:

$$\frac{1}{r}\frac{d}{dr}\left(r\frac{dT}{dr}\right) + \frac{w_b c_b \mu_p(1 + 2.5H_t)\mathrm{Re}}{k\,\vartheta\,d}(T_a - T) + \frac{q_m}{k} = 0 \tag{9}$$

2.5 Resolution Based on FDM

In this section, we are going to solve Eq. (9) numerically by using FDM.

From Eq. (9), we have:

$$\frac{d^2T}{dr^2} + \frac{1}{r}\left(\frac{dT}{dr}\right) + \frac{w_b c_b \mu_p(1 + 2.5H_t)\mathrm{Re}}{k\,\vartheta\,d}(T_a - T) + \frac{q_m}{k} = 0 \tag{10}$$

Using the FDM we can obtain the following equations:

$$\frac{\partial T}{\partial r} = \frac{T_{i+1} - T_{i-1}}{2h} \tag{11}$$

$$\frac{\partial^2 T}{\partial r^2} = \frac{T_{i+1} - 2T_i + T_{i-1}}{h^2} \tag{12}$$

with $h = \Delta r$. Now let us introduce Eqs. (11) and (12) into Eq. (10), we have:

$$\left(1 - \frac{1}{2i}\right)T_{i-1} - \left(2 + \frac{\frac{w_b c_b \mu_p(1+2.5H_t)\mathrm{Re}}{k\,\vartheta\,d}h^2}{k}\right)T_i + \left(1 + \frac{1}{2i}\right)T_{i+1} = \mathrm{F} \tag{13}$$

where $\mathrm{F} = -\frac{h^2}{k}\left(q_m + \frac{w_b c_b \mu_p(1+2.5H_t)\mathrm{Re}}{k\,\vartheta\,d}T_a\right)$.

2.6 Discretisation of Boundary Condition

This section presents the discretization of boundary condition applied in the model. According to Eq. (3) we write:

$$\text{for } i = 0: \; 2T_1 - \left(2 + \frac{\frac{w_b c_b \mu_p(1+2.5H_t)\mathrm{Re}}{k\,\vartheta\,d}h^2}{k}\right)T_0 = F \tag{14}$$

for i = 1, 2, …, R-1.

$$\left(1 - \frac{1}{2i}\right)T_{i-1} - \left(2 + \frac{\frac{w_b c_b \mu_p(1+2.5H_t)\mathrm{Re}}{k\,\vartheta\,d}h^2}{k}\right)T_i + \left(1 + \frac{1}{2i}\right)T_{i+1} = F \tag{15}$$

and for $i = R$.

$$2T_{R-1} - DT_R + E = F \tag{16}$$

with

$$D = \left[\left(2 + \frac{\frac{w_b c_b \mu_p(1+2.5H_t)\mathrm{Re}}{k\,\vartheta\,d}h^2}{k}\right) - \frac{2hh_a}{k}\left(1 + \frac{1}{2R}\right)\right]$$

and

$$E = \frac{2hh_aT_\infty}{k}\left(1 + \frac{1}{2R}\right)$$

From Eqs. (14)-(16) we can find the following system of linear equations represented in matrix form:

$$\mathrm{AX} = \mathrm{B} \tag{17}$$

where

$$A = \begin{bmatrix} a & 2 & 0 & \dots & 0 \\ b_i & a & c_i & \dots & 0 \\ 0 & b_i & a & c_i & 0 \\ \vdots & \vdots & \vdots & \ddots & \vdots \\ 0 & 0 & 0 & 2 & -D \end{bmatrix}; X = \begin{bmatrix} T_0 \\ T_1 \\ T_2 \\ \vdots \\ T_R \end{bmatrix} \text{ and } \mathrm{B} = \begin{bmatrix} F \\ F \\ F \\ \vdots \\ F - E \end{bmatrix}$$

$$\mathrm{a} = -\left(2 + \frac{\frac{w_b c_b \mu_p(1+2.5H_t)\mathrm{Re}}{k\,\vartheta\,d}h^2}{k}\right); \; b_i = \left(1 - \frac{1}{2i}\right)$$

and $c_i = \left(1 + \frac{1}{2i}\right)$ where i is the number of line .

The matrix (17) gives the nodal values in FDM which make it possible to calculate the temperature distribution profile.

2.7 Analytical Resolution

To solve analytically, we first carry out the dimensioning of Eq. (9) and its boundary condition by introducing the characteristic quantities [16, 17].

$$r^* = \frac{r}{R}\ ;\ T^* = \frac{T - T_\infty}{T_a - T_\infty} \tag{16}$$

Then, replace Eq. (16) in Eq. (9):

$$\frac{1}{r^*}\frac{d}{dr^*}\left(r^*\frac{dT^*}{dr^*}\right) + \frac{w_b c_b \mu_p (1 + 2.5H_t)\mathrm{Re}\ R^2}{k\ \vartheta\ d}(1 - T^*) + \frac{q_m R^2}{k(T_a - T_\infty)} = 0 \tag{17}$$

Here the dimensionless parameters and variables will be defined as:

$$w_b^* = \frac{w_b c_b \mu_p (1 + 2.5H_t)\mathrm{Re}\ R^2}{k\ \vartheta\ d}\ ;\ q_m^* = \frac{q_m R^2}{k(T_a - T_\infty)}\ ;\ h_A^* = \frac{h_A R}{k} \tag{18}$$

Thus Eqs. (9) and (3) can be rewritten in the form:

$$\frac{1}{r^*}\frac{d}{dr^*}\left(r^*\frac{dT^*}{dr^*}\right) - w_b^* T^* - w_b^* T^* + (w_b^* + q_m^*) = 0 \tag{19}$$

$$r^* = 0\ , \frac{dT^*}{dr^*} = 0, \text{and } r^* = 1, \frac{dT^*}{dr^*} = -h_A^* T^* \tag{20}$$

Also, in order to normalize the equation, we assume:

$$A = w_b^* + q_m^*\ , B = w_b^*\ , \varphi = A - BT^* \tag{21}$$

By thus substituting Eq. (21) in Eq. (19), we obtain:

$$\frac{d^2\varphi}{dr^{*2}} + \frac{1}{r^*}\frac{d\varphi}{dr^*} - B\varphi = 0 \tag{22}$$

It is clear that Eq. (22) is a modified zero order Bessel differential equation, the general solution of which can be expressed as follows:

$$\mathrm{R(z)} = c_1 I_v(z) + c_2 k_v(z) \tag{23}$$

where I_v and k_v are respectively the modified Bessel functions of the second type. In order to determine it, if the analytical solution can be expressed by the Bessel function, Eq. (22) was compared to the generalized Bessel equation as follows:

$$\frac{d^2R}{dx^2} + \left[\frac{1-2m}{x} - 2\alpha\right]\frac{dR}{dx} + \left[p^2a^2x^2p^{-2} + \alpha^2 + \frac{\alpha(2m-1)}{x} + \frac{m^2 - p^2v^2}{x^2}\right]R = 0 \tag{24}$$

The corresponding solution of Eq. (24) is:

$$R = x^m e^{\alpha x}[c_1 J_v(ax^p) + c_2 Y_v(ax^p)] \tag{25}$$

where J_v and Y_v are respectively the modified Bessel functions of the first type, c_1 and c_2 are arbitrary constants which can be obtained as a function of the given boundary conditions. The result of the comparison between Eqs. (22) and (24) is shown below:

$$\alpha = 0, m = 0,\ v = 0, p = 1,\ a^2 = -\beta$$

Thus, the solution of Eq. (22) can be expressed as:

$$\varphi = c_1 I_0\left(\sqrt{B}r^*\right) + c_2 K_0\left(\sqrt{B}r^*\right)) \tag{26}$$

By replacing Eq. (26) with Eq. (21), the solution of Eq. (19) can be written as:

$$T^* = \frac{w_b^* + q_m^*}{w_b^*} - \left[\frac{c_1}{w_b^*} I_0\left(\sqrt{w_b^* r^*}\right) + \frac{c_2}{w_b^*} K_0\left(\sqrt{w_b^* r^*}\right)\right] \tag{27}$$

The next step is to determine the values of two arbitrary constants c_1 and c_2.

According to the characteristics of the Bessel equation, when $z = 0$, we have:

$$I_1(0) = 0\ \ and\ \ K_1(0) \to \infty$$

Taking into account the boundary conditions of Eq. (20), simple derivations lead to:

$$c_2 = 0\ , \frac{dT^*}{dr^*} = -\frac{c_1}{w_b^*} I_1\left(\sqrt{w_b^*} r^*\right) \tag{28}$$

so we have:

$$T^*(r^*) = \left(1 + \frac{q_m^*}{w_b^*}\right)\left[1 - \frac{I_0\left(\sqrt{w_b^*} r^*\right)}{I_0\left(\sqrt{w_b^*}\right) + \frac{\sqrt{w_b^*}}{h_A^*} I_1\left(\sqrt{w_b^*}\right)}\right] \tag{29}$$

Finally, the analytical solution of T is:

$$\mathrm{T}(r^*) = T_\infty + (T_a - T_\infty)\left(1 + \frac{q_m^*}{w_b^*}\right)\left[1 - \frac{I_0\left(\sqrt{w_b^*}r^*\right)}{I_0\left(\sqrt{w_b^*}\right) + \frac{\sqrt{w_b^*}}{h_A^*} I_1\left(\sqrt{w_b^*}\right)}\right] \tag{30}$$

Table 2 Values of parameters.

Symbol	Value	Unit	Description	Reference
w_b	0.00003	kg/s·m^3	Blood perfusion	[13]
c_b	3,850	J/kg·℃	Blood specific heat	[11]
K	0.48	W/m·℃	Tissue K	[11]
h_A	30.023	W/m·℃	Heat transfer coefficient	[11] [11]
q_m	1,085	W/m^3	Heat generation per unit volume	[11] [11]
T_a	37	℃	Artery temperature	[11]
R	0.0285	m	Radius	[11]
H_t	45%	-	Hematocrite	[11]
ϑ	0.0167	m/s	Mean blood velocity	[15]
μ_p	0.165	mPas	Plasma viscosity	[15]

3. Results and Discussions

3.1 Validation of Results

The results of the new model were validated by the reproduction of the results of the literature established for a simple pipe (without stenosis and Hematocrit). In this work, we introduced the stenosis and the hematocrit, we observe the rise in temperature of 0.5 degree when r = 0. Beyond that, for an r which tends towards 0.03 we observe a convergence, this is due to the boundary condition (Fig. 3a).

Fig. 3b shows a decrease in temperature when the radial direction becomes important. This is due to the fact that when the body temperature is above the set value, the hypothalamus causes the phenomenon of sweating, evaporation, which causes a lowering of the skin temperature. At the same time, the skin arterioles dilate in order to promote heat exchanges with the outside.

3.2 Influence of Stenosis on Temperature

Fig. 4 describes the evolution of the temperature with the increasing of the stenosis size. It shows that, as the obstacle increases, the temperature increases too. This increase in temperature is due to the friction of the fluid particles. This implies that, the stress becomes important at the cross of the stenosis section and it will therefore be important to control the temperature to avoid the evolution of stenosis. In the previous work [14] it was observed that, when the stenosis increased radially, the amplitude of the oscillations decreased as the inertial blood flow decreased rapidly due to blockage of the lumen. This suggests that the loss of singular inertial blood flow occurs when there is disturbance of the normal flow.

In the same vein [18] it shows for a high temperature, more than 38 °C, the patient is victim of cardiovascular and cerebrovascular disease. This is in agreement with our result, since Fig. 4 shows that at a higher temperature of 38 °C the stenosis is already more than 50% of reduction in the initial wall.

Furthermore, in the experience of Ref. [19], they observed a rat with a body temperature above 40 °C, plunging into a brain violation in a few hours. This is in agreement with our result, since Fig. 4 shows that when the temperature is higher than 40 °C, the degree

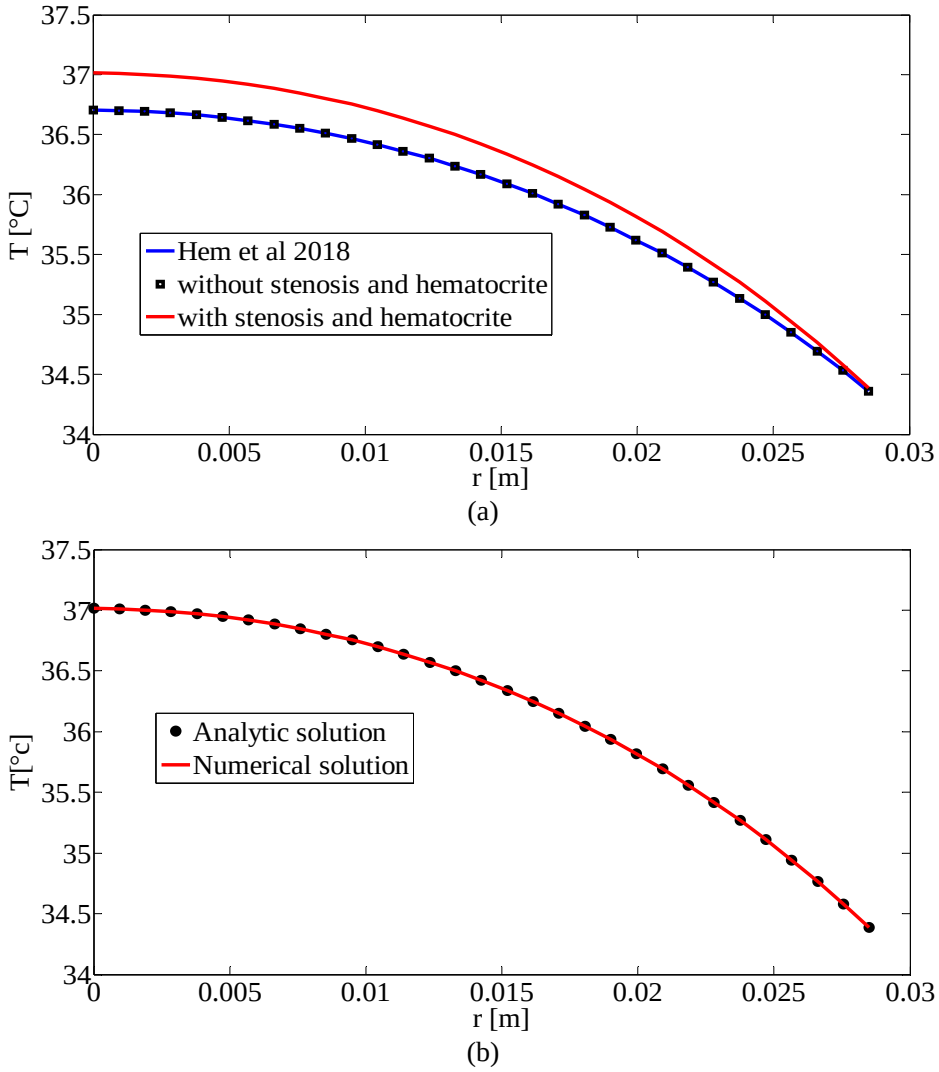

Fig. 3 Temperature as a function of the radial direction.

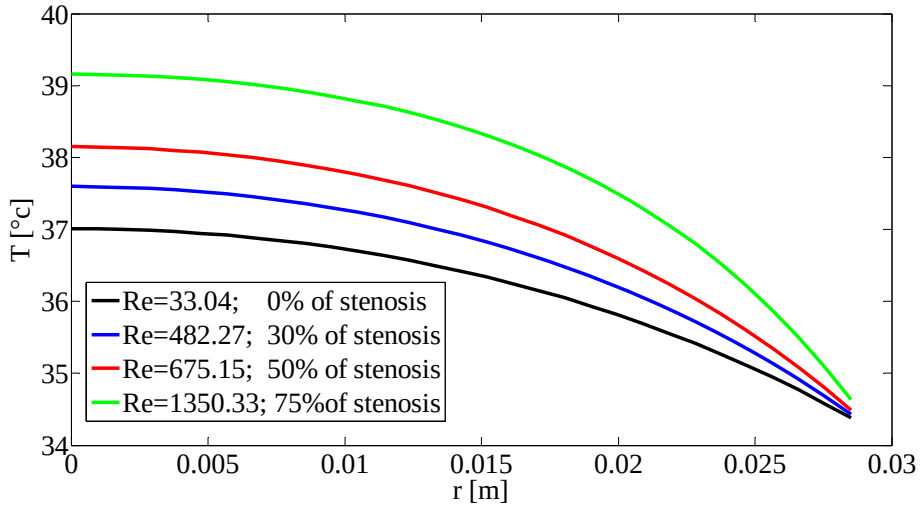

Fig. 4 Influence of stenosis on temperature.

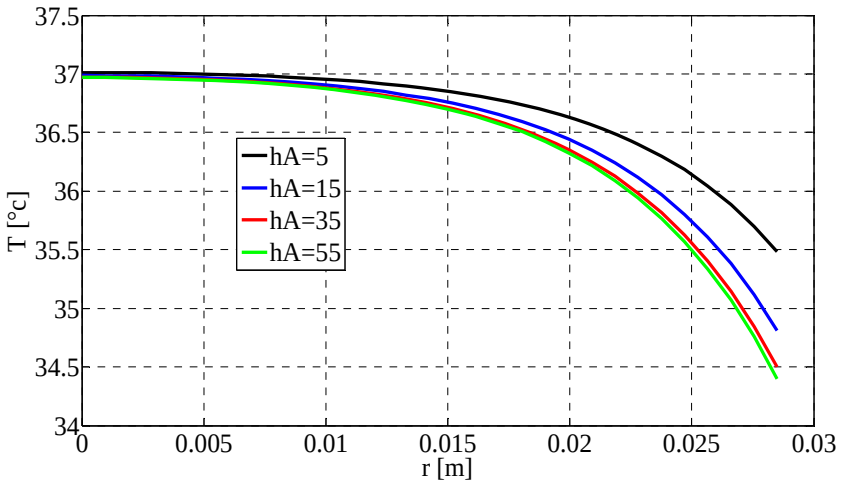

Fig. 5 Influence of the heat transfer coefficient on temperature.

of stenosis is higher than 75% of reduction of the arterial wall, therefore this is normal that, this rat is exposed to the brain offense.

3.3 Temperature Decrease Study

3.3.1 Influence of the Heat Transfer Coefficient

Fig. 5 shows that increasing the heat transfer coefficient decreases body temperature. This is because the temperature of the atmospheric pressure cools the body surface. For example convection is the transfer of heat to the air surrounding the skin. The warmed air rises away from the body and is replaced by cooler air that is subsequently heated. Convection can also occur in water when the water temperature is lower than the body's temperature, the body loses heat by warming the water closet to the skin, which moves away to be replaced by cooler water. The convection current created by the temperature changes continues to draw heat away from the body more quickly than the body can replace it, resulting in hyperthermia. About 15% of the body's heat is lost through convection to finish heat flow from a higher concentration to a lower concentration.

3.3.2 Influence of *K*

The result of Fig. 6 shows that the *K* has the effect of lowering the temperature. This decrease in temperature is because the atmospheric air touches the body at a lower temperature. According to Fourier law, the temperature moves from the hottest medium to the least hottest medium. For example conduction is the transfer of heat by two objects that are in direct contact with one another. It occurs when the skin comes in contact with a cold or worm object. For example, when holding a glass of ice water, the heat from your skin will warm the glass and in turn melt the ice. Alternatively, on a cold day, you might warm up by wrapping your cold hand around a hot mug of coffee. Only about 3% of the body's heat is lost through conduction.

3.4 Study of an Increase of Temperature

3.4.1 Influence of Ht (Hematocritis)

The result of Fig. 7 shows that, the increase of hematocrit increases the body temperature; this is due to the fact that, the hematocrit increases the density of the blood, and that provokes an increase in resistance of the blood flow [14, 20].

3.4.2 Influence of the Generation of heat Metabolic (qm)

Fig. 8 shows that, increasing qm increases the temperature. This is due to the fact that the metabolic generates heat, which causes the body temperature to rise. In the process of ATP production by cells throughout the body, approximately 60% of the energy produced is in the form of heat used to maintain body temperature.

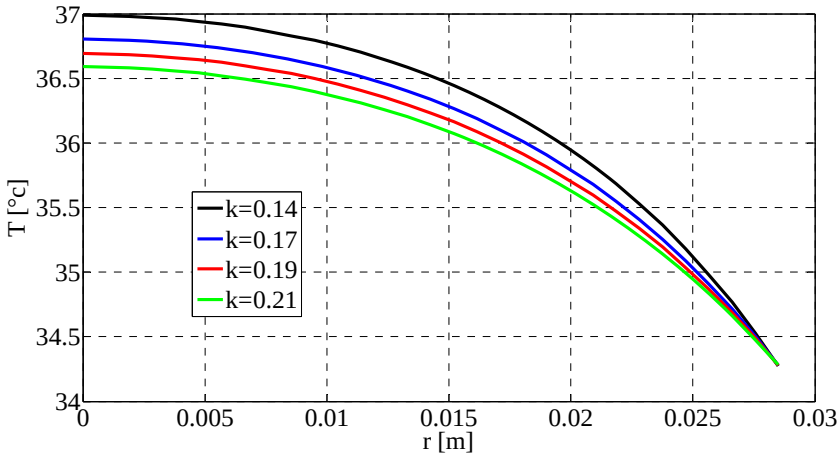

Fig. 6 Influence of *K* on the temperature.

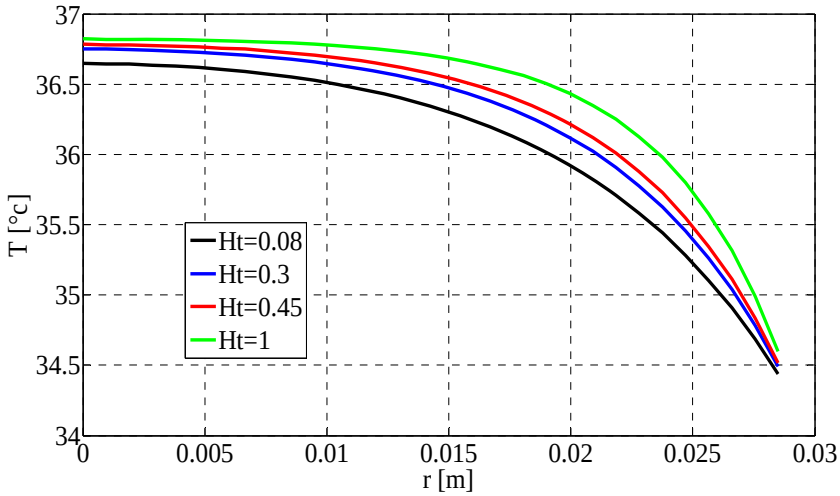

Fig. 7 Influence of Ht on the temperature.

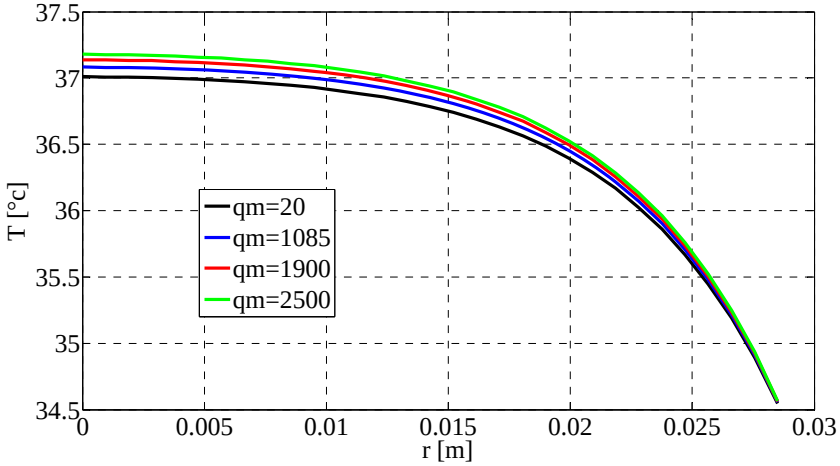

Fig. 8 Influence of the generation of qm (metabolic charger) on temperature.

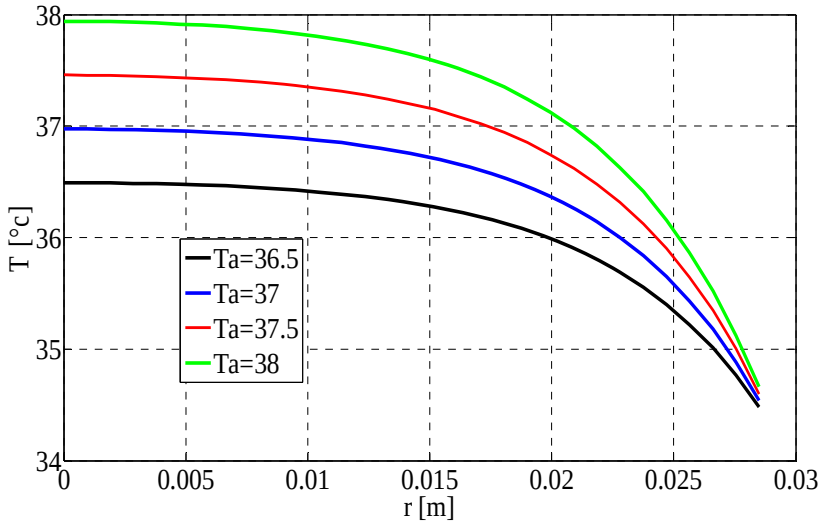

\

Fig. 9 Influence of T_a (arterial temperature) on the skin temperature.

3.4.3 Influence of T_a

Fig. 9 shows that increasing T_a increases body temperature. Furthermore we observe that the T_a is equal to the body temperature (T_a = 36.5, 37, 37.5, 38 °C is equal to body temperature T = 36.5, 37, 37.5, 38 °C respectively).

4. Conclusion

In this article we have studied the distribution of the temperature of biological tissue, taking into account stenosis and hematocrit. The heat transfer model of Penne in one-dimensional biological heat transfer in steady state has been solved by the numerical and analytical method, to obtain the temperature changes with variation in the size of the stenosis and hematocrit. The results of this contribution brought a new technic to use temperature to control the evolution of stenosis; this is to improve the prediction of cardiovascular and cerebral diseases. The results provided by this article promote the knowledge to control the evolution size of stenosis by taking just a temperature of the body. These provide a good knowledge of the thermal behavior of biological tissue, which is precious for the measurement of thermal parameters, the reconstruction of a temperature field and the diagnosis and treatment of cardiovascular and cerebral disease.

References

[1] Pennes, H. H. 1948. “Analysis of Tissue and Arterial Blood Temperature in Resting Human Forearm.” *A Journal of Applied Physiology* 1 (2): 657-78.

[2] Mitchell, J. W., and Myers, G. E. 1968. “An Analytical Model of the Countercurrent Heat Exchange Phenomena.” *Biophysics Journal* 8: 897-911.

[3] Keller, K. H., and Seilder, L. 1971. “An Analysis of Peripheral Heat Transfer in Man.” *Journal of Applied Physiology* 30: 779-89.

[4] Wulff, W. 1974. “The Energy Conservation Equation for Living Tissue.” *IEEE Transactions on Biomedical Engineering* 21: 494-5.

[5] Chen, M. M., and Holmes, K. R. 1980. “Micro-vascular Contributions in Tissue Heat Transfer.” *Annals of the New York Academy of Sciences* 335: 137-50.

[6] Weinbaum, S., and Jiji, L. M. 1985. “A New Simplified Bioheat Equation for the Effect of Blood Flow on Local Average Tissue Temperature.” *ASME Journal of Biomechanical Engineering* 107: 131-9.

[7] Khaled, A.-R. A., and Vafai, K. 2003. “The Role of Porous Media in Modeling Flow and Heat Transfer in Biological Tissues.” *International Journal of Heat Mass Transfer* 46: 4989-5003.

[8] Nakayama, A., Kuwahara, F., and Liu, W. 2008. “A Macroscopic Model for Countercurrent Bioheat Transfer in a Circulatory System.” *Journal of Porous Media* 12: 289-300.

[9] Cooper, T. E., and Trezek, G. J. 1972. “A Probe Technique for Determining the Thermal Conductivity of Tissue.” *J. Heat Transfer* 94: 133.

[10] Gurung, D. B. 2007. “Mathematical Study of Abnormal Thermoregulation in Human Dermal Parts.” Ph.D. thesis,

Kathmandu University.

[11] Hen pandey, R., Gurung, D. B., and Dhulikhel., N. E. P. A. L. 2018. "Numerical Solutions of One-Dimensional Bioheat Transfer Equation in Cylindrical Living Tissues." *International Journal of Advanced Engineering Research and Application* 4 (8).

[12] Zhang, K. Y. X., and Yu, F. 2004. "An Analytic Solution of One-Dimensional Steady-State Pennes Bioheats Transfer Equation in Cylindrical Coordinates." *Journal of Thermal Science* 13 (3): 255-8.

[13] Yue, K., Zhang, X., and Yu, F. 2004. "An Analytic Solution of One-Dimensional Steady-State Pennes' Bioheat Transfer Equation in Cylindrical Coordinates." *Journal of Thermal Science* 13 (3): 255-8.

[14] Tsafack Zifack, J. R., Mabekou Takam, J. S., Fogue, M., and Talla, P. K. 2019. "Study of Cerebral Blood Flow by the Lumped Parameter Model to Predict the Rupture of the Arterial Wall: Application to Stroke." *International Journal of Academic Research and Reflection* 7 (6): 114.

[15] Rizzini, M. L. 2018. "Impact of Stenosis Length and Severity on Clinical Functional Parameters in an Atherosclerotic Coronary Model." Master thesis in Biomedical Engineering.

[16] Ozisik, M. N., and Yu, C. M. 1983. *Heat Conduction.* Beijing: Higher Education Press, 712-5.

[17] Wang, B. X., and Wang, Y. M. 1992. "Study on the Basic Equations of Biomedical Heat Transfer." In *Transport Phenomena Science and Technology*. Beijing: Higher Education Press, 773-6.

[18] Grau, A. J., Buggle, F., Schnitzler, P., Spiel, M., Lichy, C., and Hacke, W. 1999. "Fever and Infection Early after Ischemic Stroke." *J. Neurol. Sci.* 171: 115-20.

[19] Kim, Y., Busto, R., Dietrich, W. D., Kraydieh, S., and Ginsberg, M. D. 1996. "Delayed Postischemic Hyperthermia in Awake Rats Worsens the Histopathological Outcome of Transient Focal Cerebral Ischemia." *Stroke* 27: 2274-81.

[20] Verma, N., Liu, M., Ly, H., Loria, A., Campbell, K. S., Bush, H., and Despa, S. 2020. "Diabetic Microcirculatory Disturbances and Pathologic Erythropoiesis Are Provoked by Deposition of Amyloid-Forming Amylin in Red Blood Cells and Capillaries." *Kidney International* 97 (1): 143-55.